Ultrafast dynamics of femtosecond laser-induced nanostructure formation on metals

Taek Yong Hwang, A. Y. Vorobyev, and Chunlei Guo

Citation: Appl. Phys. Lett. **95**, 123111 (2009); doi: 10.1063/1.3222937
View online: http://dx.doi.org/10.1063/1.3222937
View Table of Contents: http://apl.aip.org/resource/1/APPLAB/v95/i12
Published by the American Institute of Physics.

Ultrafast dynamics of femtosecond laser-induced nanostructure formation on metals

Taek Yong Hwang, A. Y. Vorobyev, and Chunlei Guo[a)]
The Institute of Optics, University of Rochester, Rochester, New York 14627, USA

(Received 1 May 2009; accepted 16 August 2009; published online 23 September 2009)

We perform a comparison study on femtosecond laser-induced nanostructures on three noble metals, Cu, Ag, and Au. Under identical experimental conditions, the three metals each gain a different amount of surface area increase resulting from nanostructuring. We show that the different surface area increase from nanostructuring directly relates to the competition of two ultrafast processes, electron-phonon coupling and hot electron diffusion, following femtosecond laser heating of metals. © *2009 American Institute of Physics*. [doi:10.1063/1.3222937]

Nanoscale metallic structures have been studied extensively in the past due to their unique properties associated with applications such as modifying optical properties and excitation of localized surface plasmons.[1–3] With advancements of the femtosecond (fs) laser, nanostructures have been produced on metal surfaces with fs laser pulses.[3–9] For example, nanostructures have been produced on metal surfaces by using a near-field optical microscope combined with fs laser pulses.[4] Nanostructures have also been generated through the plume deposition of laser ablated material.[5,6] Recently, we showed that, under certain experimental conditions, surface nanostructures can be directly produced on metals with fs laser pulses.[3,7] These directly produced nanostructures play an important role in modifying properties of the metal surfaces significantly, contributing to the creation of the so-called black and colored metals.[3,8] Furthermore, fs laser-induced nanostructures increase the surface area of the metal. This increased surface area is also important in improving the efficiency of the metal as a catalyst.[7] In many of these applications, the control of size, density, and shape of the nanostructures is crucial in achieving the desired results. Therefore, it is important to understand the physics and ultrafast dynamics for the direct nanostructuring following fs pulse irradiation.

In this work, we perform a comparison study on fs laser-induced nanostructures on three noble metals, Cu, Ag, and Au. Under identical experimental conditions, the three metals each gain a different amount of surface area increase from the nanostructuring. We show that the different surface area increase directly relates to the competition of two ultrafast processes, electron-phonon coupling and hot electron diffusion, following fs laser heating of metals.

The laser used in this experiment is an amplified Ti:sapphire fs laser system that generates 60 fs pulses of an energy of 1.1 mJ/pulse with a 1 kHz repetition rate at a central wavelength of 800 nm. We prepare Au, Ag, and Cu samples by mechanically polishing the surfaces with 0.3-μm-grade aluminum oxide powder. To produce nanostructures, a linearly polarized fs laser beam is weakly focused onto the sample surface at normal incident. Each time, a train of laser pulses is used to irradiate the sample and the number of the pulses is controlled by an electromechanical shutter. The surface morphology of the processed samples is studied with a scanning electron microscope (SEM).

We start by studying the evolution of structural formation following sequential pulse irradiation on the three noble metals at fluence of 0.51 J/cm^2. Following a single pulse irradiation, some nanostructures are formed around the central region of the beam spot and usually around initial surface defects that help localize energy absorption. As the pulse number increases, the size of each nanostructure increases and the area covered with nanostructures also expand. Figure 1 shows the irradiated Cu, Ag, and Au surfaces following a train of 16 laser pulses. We see several types of nanostructures uniformly formed on all three noble metal surfaces. Nanodroplets spread out on the surface mostly with the size up to 250 nm in diameter; droplets larger than 250 nm are rarely seen. Another type of pronounced structure is cellular structure, typically consisting of nanorims and nanoprotrusions that surround a flat surface area of less than 1 μm^2. All the surface nanostructures will significantly increase the surface area. In thermodynamics, we know that a surface area increase associates with the excess surface internal energy U^s. Using the Gibbs convention, the volume of the interface is zero. The change in excess surface internal energy ΔU^s for a single species and under the isothermal expansion can be defined as $\Delta U^s = \sigma \Delta A^s = [\gamma - T^s(\partial\gamma/\partial T^s)_{A^s}]\Delta A^s$, where γ is the surface tension, ΔA^s is the change in the surface area, and T^s is the temperature at the surface for constant A^s.[9] Therefore, it requires a $\sigma \cdot C^* \pi w^2$ amount of excess surface internal energy to form a nanodroplet with a diameter of w, where C^* is a scaling parameter for the surface area that depends on the shape of nanodroplets. The scaling factor is 1 if the nanodroplet is a perfect sphere detached from the surface, while the value will change as the droplet deviates from a perfect sphere. In this paper, we assume that C^* is the same for all three noble metals.

Figure 2 shows the size distribution of nanodroplets from 20 up to 250 nm, divided into five size groups. For all the five size groups, Cu has a higher number density of nanodroplets than Ag and Au. Based on this observation, we can estimate the total energy required to produce nanodroplets if we assume the shape of all nanodroplets is sphere. With this assumption and using values in Table I, the ratio of the required excess surface internal energy increase to generate nanodroplets is $\Delta U^s{}_{\mathrm{Cu}} : \Delta U^s{}_{\mathrm{Ag}} : \Delta U^s{}_{\mathrm{Au}} \approx 1 : 0.47 : 0.38$

[a)]Electronic mail: guo@optics.rochester.edu.

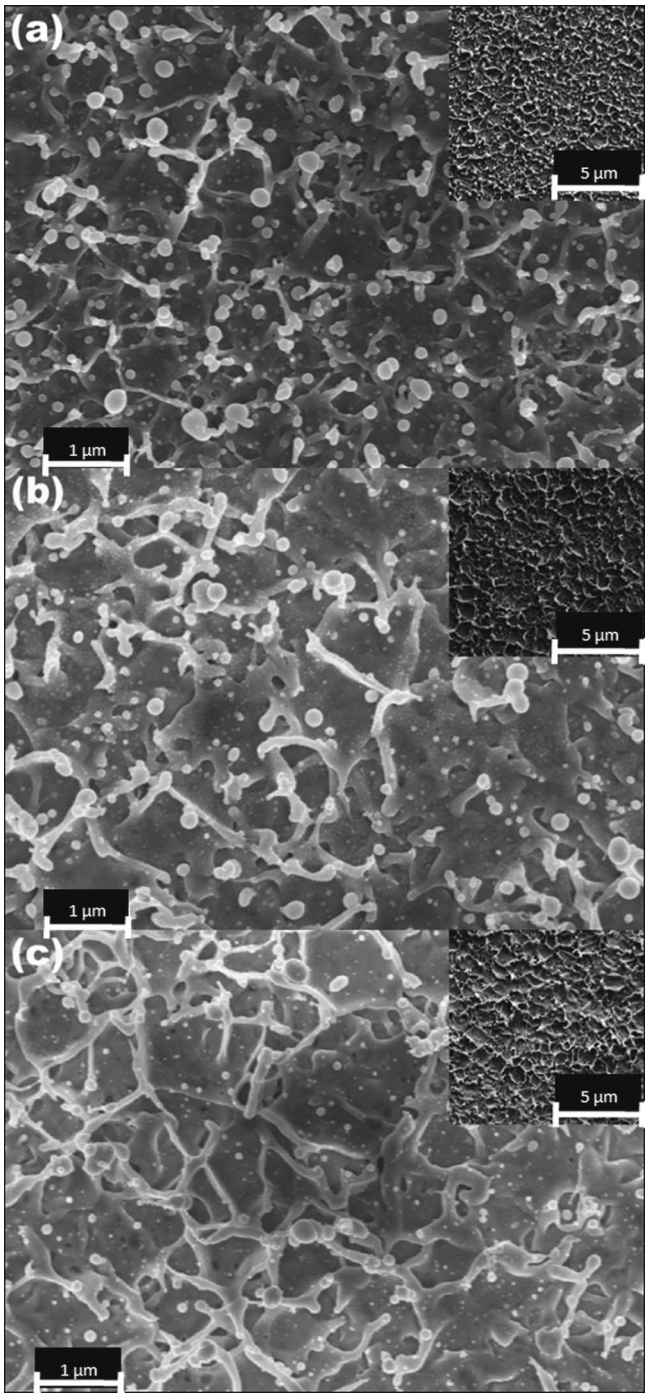

FIG. 1. SEM images of nanostructures on (a) Cu, (b) Ag, and (c) Au in the central region of the Gaussian beam spot following 16 laser pulse irradiations at fluence of 0.51 J/cm^2.

$(\Delta A^s{}_{Cu}:\Delta A^s{}_{Ag}:\Delta A^s{}_{Au} \approx 1:0.61:0.47)$. Besides nanodroplets, Cu surface also shows the highest density of nanostructure aggregation, especially the cellular structures as shown in Fig. 2. The average size of the cell structures on Cu, Ag, and Au is about 0.33, 0.51, and 0.68 μm^2, respectively. Therefore, the ratio of the surface area increase due to the cell structures for Cu, Ag, and Au is $\Delta A^s{}_{Cu}:\Delta A^s{}_{Ag}:\Delta A^s{}_{Au} \approx 1:0.77:0.67$ by assuming that the cell structures consist of two-dimensional sinusoidal-wave structures with the same amplitude but different period that each is proportional to the square root of the average area size. Accordingly, the ratio of excess surface internal energy increase due to the cell structures is $\Delta U^s{}_{Cu}:\Delta U^s{}_{Ag}:\Delta U^s{}_{Au} \approx 1:0.59:0.54$, and this ratio is similar to that of the nanodroplets. Based on this observation, Cu requires the highest amount of excess energy among the three noble metals. However, if we assume the depth of the melting layer is the same for the three metals, Cu will require the highest laser fluence to melt while Au will require the least.[10] This suggests that the least amount of energy will be left in Cu after the absorbed energy induces the solid to liquid phase transition. This is at odds with the analysis above where Cu needs to have the greatest amount of excess surface internal energy to induce the largest surface area change. Therefore, other physical mechanisms need to be carefully considered to understand these experimental results.

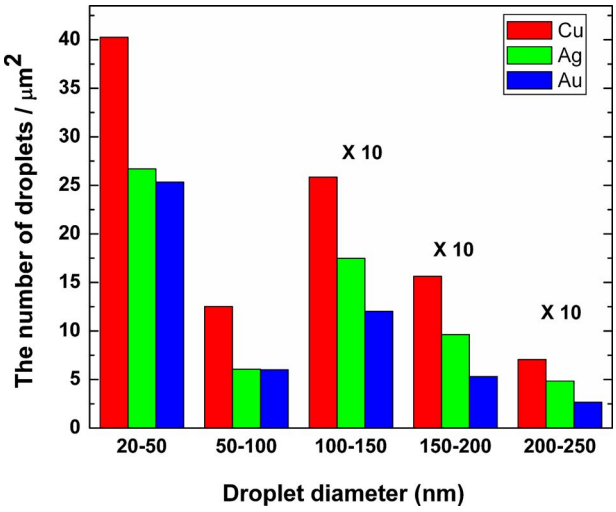

FIG. 2. (Color online) The size distribution of nanodroplets on Cu, Ag, and Au surfaces. The densities of nanodroplets larger than 100 nm are scaled up by ten times.

Our understanding of fs laser interactions with metals is largely based on the so-called two-temperature model (TTM).[11,12] Since the heat capacity of the electrons in a metal is much smaller than that of the lattice, an ultrashort laser pulse can heat electrons to a very high temperature while leaving the lattice relatively cool. In most cases, the thermalization of the hot electrons can be assumed to occur instantaneously due to the short electron-electron interaction time.[12] Therefore, the overall picture of a nonequilibrium system in metals is normally described as constituting two subequilibrium systems, the hot electrons and a cold lattice.[13] This transient two-temperature system will tend to reach equilibrium within a few picoseconds through electron-phonon interactions as well as electrons diffuse out of the excited region.[12–14] This dynamic process can be described by the following TTM:[12]

TABLE I. Material constants for Cu, Ag, and Au (Refs. 15 and 17–19).

	Cu	Ag	Au
$g(10^{16}\ W/m^3\cdot K)$	10	3.6	2.1
$K_{e0}(=K_e\cdot T_l/T_e)(W/m\cdot K)$	401	429	318
$C_{e0}(=C_e/T_e)(J/m^3\cdot K^2)$	90	66	70
$C_l(10^6\ J/m^3\cdot K)$	3.44	2.47	2.49
$\sigma(mN/m)$	1727	1337	1403
$d\gamma/dT(mN\ m^{-1}\ K^{-1})$	−0.26	−0.21	−0.18

$$C_e \frac{\partial T_e}{\partial t} = \nabla(K_e \nabla T_e) - g(T_e - T_l) + A(r,t),$$

$$C_l \frac{\partial T_l}{\partial t} = g(T_e - T_l), \quad (1)$$

where C_e and C_l are the electron and lattice heat capacity, K_e is the electron thermal conductivity, g is the electron-phonon coupling coefficient, T_e and T_l are the electron and lattice temperatures, respectively, and $A(r,t)$ is the external energy source.

For the three noble metals, all the parameters in Eq. (1) have approximately the same values (all within 35%) except for g, as shown in Table I. The time evolution of electron and lattice temperatures for Cu, Ag, and Au before thermal equilibrium is mostly governed by the g parameter. For a larger g, electrons transfer more energy locally to the adjacent lattice, and the lattice near the surface will tend to reach a higher temperature before hot electrons diffuse into the sample from the surface. This has been confirmed by some of our previous numerical simulations for the three noble metals.[15] Furthermore, a large g factor also leads to more localized energy absorption. Since melting often starts from strong energy deposition around isolated surface defects, a larger g factor will enhance the energy localization around initial surface defects.[15] Consequently, a larger g factor helps local heat accumulation to reach melting threshold, resulting in a greater number of local melts. Moreover, the stronger nonuniform temperature distribution around local melting spots will induce a greater surface tension gradient or Marangoni force, $\nabla_s \gamma(T)$, where ∇_s is the surface gradient and T is the temperature.[16] Therefore, within a pot of locally melted liquid metal, a larger g factor also leads to a greater Marangoni force that will push the liquid metal to a lower temperature region. This will lead to a greater amount of liquid metal flow and eventually result in more nanostructures and a greater surface area increase for a larger g factor. As shown in Table I, electron-phonon energy coupling coefficient g for Cu, Ag, and Au are 10×10^{16}, 3.6×10^{16}, 2.1×10^{16} $\mathrm{W/m^3\,K}$, respectively. Therefore, we expect that surface area increase will be greatest for Cu, less for Ag, and least for Au, and this is clearly consistent with our experimental observation. Note that Eq. (1) shows that parameters other than the g parameter, including thermal conductivities and heat capacities, also play a role in determining final surface temperature nonuniformity. However, as we mentioned earlier, all the other parameters have approximately the same values (all within 35%) except for g, as shown in Table I. To confirm that the g factor indeed plays the dominant role, we recently performed systematic calculations to isolate effects of different parameters on the final lattice temperature distribution for the three noble metals. Our calculations showed that the g parameter plays the dominant role in determining the final surface temperature nonuniform, and the effects of thermal conductivity and heat capacity are relatively unimportant for comparison among Cu, Ag, and Au.[15]

In summary, we perform a comparison study on fs laser-induced nanostructures on three noble metals, Cu, Ag, and Au. Under identical experimental conditions, our results show that the three metals each gain a different amount of surface area increase from the nanostructure formation. We show that the different surface area increase from nanostructuring directly relates to the competition of two ultrafast processes, electron-phonon coupling and hot electron diffusion, following fs laser heating of metals.

We thank J. Wang, A. Heins, and H. Shin for discussions and technical assistance. This work was supported by the U.S. Air Force Office of Scientific Research.

[1] U. Kreibig and M. Vollmer, *Optical Properties of Metal Clusters* (Springer, Berlin, 1995).
[2] S. A. Maier, *Plasmonics: Fundamentals and Applications* (Springer, New York, 2007).
[3] A. Y. Vorobyev and C. Guo, Appl. Phys. Lett. **92**, 041914 (2008).
[4] S. Nolte, B. N. Chichkov, H. Welling, Y. Shani, K. Liebermann, and H. Terkel, Opt. Lett. **24**, 914 (1999).
[5] S. Eliezer, N. Eliaz, E. Grossman, D. Fisher, I. Gouzman, Z. Henis, Y. Horovitz, M. Frankel, S. Maman, and Y. Lereah, Phys. Rev. B **69**, 144119 (2004).
[6] S. Amoruso, G. Ausanio, R. Bruzzese, M. Vitello, and X. Wang, Phys. Rev. B **71**, 033406 (2005).
[7] A. Y. Vorobyev and C. Guo, Opt. Express **14**, 2164 (2006).
[8] A. Y. Vorobyev and C. Guo, Appl. Phys. Lett. **86**, 011916 (2005).
[9] H. Yildirim Erbil, *Surface Chemistry of Solid and Liquid Interfaces* (Blackwell, Oxford, 2006).
[10] J. Wang and C. Guo, Appl. Phys. Lett. **87**, 251914 (2005).
[11] S. I. Anisimov, B. L. Kapeliovich, and T. L. Perel'man, Zh. Eksp. Teor. Fiz. **66**, 776 (1974).
[12] J. G. Fujimoto, J. M. Liu, E. P. Ippen, and N. Bloembergen, Phys. Rev. Lett. **53**, 1837 (1984).
[13] G. L. Eesley, Phys. Rev. Lett. **51**, 2140 (1983).
[14] H. E. Elsayedali, T. B. Norris, M. A. Pessot, and G. A. Mourou, Phys. Rev. Lett. **58**, 1212 (1987).
[15] J. Wang and C. Guo, J. Appl. Phys. **102**, 053522 (2007).
[16] R. F. Probstein, *Physicochemical Hydrodynamics: An Introduction* (Wiley, New York, 1994).
[17] J. Hohlfeld, S.-S. Wellershoff, J. Gudde, U. Conrad, V. Jahnke, and E. Matthias, Chem. Phys. **251**, 237 (2000).
[18] D. R. Lide, *CRC Handbook of Chemistry and Physics*, 82nd ed. (CRC, Boca Raton, 2002).
[19] B. J. Keene, Int. Mater. Rev. **38**, 157 (1993).